The influence of cation additives on the NIR luminescence intensity of Er^{3+}-doped borate glasses*

Zhou Yong-Liang(周永亮), Zhang Xiao-Song(张晓松),
Xu Jian-Ping(徐建萍), Zhang Zhong-Peng(张忠朋),
Zhang Gao-Feng(张高峰), Wei Feng-Wei(魏凤巍), and Li Lan (李 岚)†

Institute of Material Physics, Key Laboratory of Display Materials and Photoelectric Devices, Ministry of Education, Tianjin University of Technology, Tianjin 300384, *China*

(Received 12 August 2011; revised manuscript received 16 February 2012)

Er^{3+}-doped 25BaO-(25-x)SiO_2-xAl_2O_3-25B_2O_3 transparent glasses are prepared with x = 0, 12.5 and 25 by a solid-state reaction. The Er-related NIR luminescence intensity, which corresponds to the transition of $^4I_{15/2}$–$^4I_{13/2}$, is obviously altered with different silicon/aluminum ratios. The Judd–Ofelt parameters of the Er^{3+} ions are adopted to explain the intensity change in the NIR fluorescence, and the Raman scattering intensity versus the amount of Al and/or Si components are discussed. The spectra of the three samples are quite similar in the peak positions, but different in intensity. The maximal phonon density of state for the samples is calculated from the Raman spectra and is correlated to the NIR luminescence efficiency.

Keywords: maximal phonon density of state, Judd–Ofelt intensity parameter, Er^{3+}-doped borate glasses

PACS: 63.20.–e, 95.30.ky, 64.70.ph **DOI:** 10.1088/1674-1056/21/6/066301

1. Introduction

Due to near-infrared ray (NIR) luminescence (centered at around 1540 nm) covering the important optical communication windows from the $^4I_{13/2}$–$^4I_{15/2}$ transition of Er^{3+}, Er^{3+}-doped borate glasses are of great interest for applications in solid-state glass lasers and fiber lasers.[1–3] The Er^{3+} concentration and local ligand crystal field are considered as two distinct and strong factors towards achieving high output efficiency, good beam quality, and weak temperature dependence.[4–6] But an excessive concentration over 4 mol% of the Er^{3+}-doped phosphate glasses leads to a reduction in the transition probability $^4I_{13/2}$–$^4I_{15/2}$ of Er^{3+} because of concentration quenching and nonradiative transition.[7] Noting that the probability of radiative transition and nonradiative relaxation were affected by crystal field symmetry and the strength around the rare-earth ion, the incorporation of guest-ions such as Al^{3+} and B^{3+} caused an enhancement in the crystal field strength of the oxygen coordination structure surrounding Eu^{3+} ions, and an improved luminescence efficiency of Y_2O_3:Eu^{3+}.[8] Considering the similar electronegativity and ionic radius between Al^{3+} and Si^{4+}, it was reported that the replacement of Al^{3+} by Si^{4+} in the YAG:Ce^{3+} phosphor could increase the level splitting of Ce^{3+} and reduce the radiative transition probability.[9] The substitution of doping ions in the host lattice, inducing local distortions and changing the local crystal field symmetry of active ions, has a significant influence on the luminescent properties of the material.

As a nondestructive technique, Raman scattering spectroscopy can be used to determine the interaction between photons and high-frequency optical phonons caused by the vibration of molecules and atoms in rare-earth-doped glass materials.[10,11] Considering the multi-phonon decay of rare-earth ions in a glass, which depends on the maximum phonon energy of the host glass,[12,13] Kishimoto and Hirao[14] explained the enhancement of UV-emission intensity and the blue up-conversion luminescence of Tm^{3+} by phonon sideband spectroscopy. For most matrices with similar phonon energies, multi-phonon decay ef-

*Project supported by the Natural Science Foundation of Tianjin (Grant Nos. 09JCYBJC01400 and 11JCYBJC00300), the Natural Science Foundation of the Tianjin Education Committee (Grant No. 20071207), and Tianjin Key Subject for Materials Physics and Chemistry.

†Corresponding author. E-mail: lilan@tjut.edu.cn

© 2012 Chinese Physical Society and IOP Publishing Ltd

ficiencies for RE^{3+} ions, which have a correlation with the radiative transition probability of the excited upper level, are obviously different owing to differences in the phonon density of state.[15] However, researchers seldom pay attention to whether phonon density diversification has an influence on the luminescent properties in the course of ion replacement.

In this paper, Er^{3+}-doped 25BaO-(25-x)SiO_2-xAl_2O_3-25B_2O_3 transparent glasses were prepared by a solid-state reaction. The melting temperature was determined by thermal mechanical analysis, and the amorphous structure was characterized with X-ray diffraction (XRD) analysis. The influence of Si^{4+} and/or Al^{3+} addition on the infrared fluorescence properties of Er^{3+} ions was investigated. The luminescence intensity parameters, Ω_2, of the Er^{3+} ions calculated by Judd–Ofelt theory, which is related to the local crystal field symmetry of Er^{3+} ions, were used to explain the luminescence intensity difference of the samples. The microstructures were investigated by Raman spectra and the obtained phonon density of state was used to explain the correlation between the altered environment of the Er^{3+} ions for Si^{4+} and/or Al^{3+} addition and infrared luminescence properties.

2. Experimental details

Analytically pure powders of $BaCO_3$, SiO_2, Al_2O_3, H_3BO_3, and $Er(CH_3COO)_3$ were used as starting materials. The samples were prepared with nominal molar compositions of 25BaO-(25-x)SiO_2-xAl_2O_3-25B_2O_3:0.5Er^{3+} (x = 0, 12.5, 25), and the detailed compositions are listed in Table 1.

Table 1. Composition of the prepared samples.

Samples	Ingredient/mol%				
	$BaCO_3$	Al_2O_3	SiO_2	H_3BO_3	$Er(CH_3COO)_3$
BSB	25	0	25	50	0.5
BASB	25	12.5	12.5	50	0.5
BAB	25	25	0	50	0.5

The starting materials were milled completely and then sintered in an aluminum crucible at the temperature, which was determined by the method of differential thermal analysis.

The differential thermal analysis (DTA) and thermogravimetric analysis (TGA) were obtained using a SHIMADZU DTG-60H thermal analyzer operating at ramp 10 °C/min from room temperature to 900 °C. The absorption spectra of the samples were taken by the Hitachi U-4100 UV absorption spectrophotometer. X-ray power diffraction (XRD) patterns were characterized on a Bruker D8 advance X-ray diffractmeter with Cu Kα radiation (λ = 1.5418 Å, 1 Å = 0.1 nm). The infrared fluorescence spectra were observed under excitation wavelength at 980 nm by a Jobin Yvon FL3-221-TCSPC fluorescence spectrophotometer, and the Raman scattering spectra were recorded by a Thermo-Fisher Scientific DXR Laser Raman spectroscope. All the spectra were carried out at room temperature.

3. Results and discussion

Figure 1 shows TGA and DTA curves of the precursor mixture of $BaCO_3$, SiO_2, and H_3BO_3. Also, the differential thermogravimetric (DTG) curve was derived from the TGA curve and displayed in Fig. 1. For the overall temperature range, the DTA curve exhibits five obvious endothermic peaks, corresponding to 89 °C, 136 °C, 169 °C, 682 °C, 735 °C. The temperature of 89 °C at the low temperature range usually suggests the desorption of water molecules[16], and the two peaks at 136 °C and 169 °C are attributed to the thermal decomposition of boric acid.[17] An inconspicuous shoulder appears at a temperature of 480 °C, which can be regarded as glass transition temperatures (T_g). For the high temperature range, the two endothermic peaks at 682 °C and 735 °C, corresponding to the small weight losses observed in the TGA curve, indicate the reaction between SiO_2 and $BaCO_3$ or H_3BO_3. Yun[18] proposed that the formation of the $[BSi_4O_{10}]^{-1}$ unit was at the expense of H_3BO_3 and SiO_2 at temperatures above 600 °C. And the barium orthosilicate (Ba_2SiO_4) is generally considered to be the product of the solid state reaction between $BaCO_3$ and SiO_2 at 730 °C–750 °C.[19]

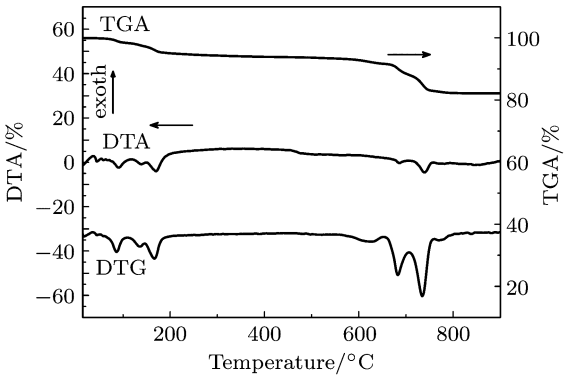


Fig. 1. The DTA and TGA curves of $BaCO_3$, SiO_2, H_3BO_3.

The formation of the Si-related groups can be achieved by chemical reaction as follows:

$$[BO_4]^{-1} + 4SiO_2 \rightarrow [BSi_4O_{10}]^{-1} + O_2,$$

$$2BaCO_3 + SiO_2 \rightarrow Ba_2SiO_4 + 2CO_2.$$

The relatively higher temperature that is sufficient to melt the mixture was chosen to be 1100 °C. 510 °C was determined as the annealing temperature to exclude stress and air bubbles.

The absorption spectra in the UV-NIR range are shown in Fig. 2. For all samples, the observed four main absorption peaks at 378 nm, 518 nm, 650 nm, and 1534 nm can be attributed to the transition of $^4I_{15/2}$–$^4G_{11/2}$, $^4I_{15/2}$–$^2H_{11/2}$, $^4I_{15/2}$–$^4F_{9/2}$, and $^4I_{15/2}$–$^4I_{13/2}$ for Er^{3+} ions, respectively.

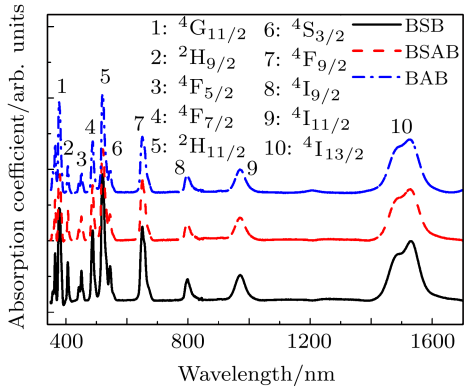


Fig. 2. (colour online) The absorption spectra for glass samples denoted as BSB, BSAB, and BAB. All the transitions involving upper energy levels are listed.

Figure 3 shows the XRD patterns of the Er^{3+}-doped 25BaO-(25-x)SiO_2-xAl_2O_3-25B_2O_3 samples for x = 0, 12.5, and 25. There are no significant differences in the XRD spectra for all the samples. Two envelope curves indicate that the samples are not fully crystallized and are in amorphous form or a glassy state.

The NIR luminescent spectra of all the samples are shown in Fig. 4(a) under an excitation wavelength of 980 nm. The sample with Al 25% doping yields the stronger emission intensity, but a relatively weaker emission is observed for the other two samples. Figure 4(b) represents a schematic energy level diagram for Er^{3+} emission. The electrons on the ground level of Er^{3+} ions can be excited to the $^4I_{11/2}$ level by 980-nm light, and then rapidly relax and populate the $^4I_{13/2}$ level. The other possible route for the excited state electrons of the $^4I_{11/2}$ and $^4I_{13/2}$ level could be reexcited to higher energy levels such as $^4F_{7/2}$ and $^4F_{9/2}$. Subsequent up-conversion emission at 540 nm from $^4S_{3/2}$ to $^4I_{15/2}$ is also observed, which will not be discussed in this paper.

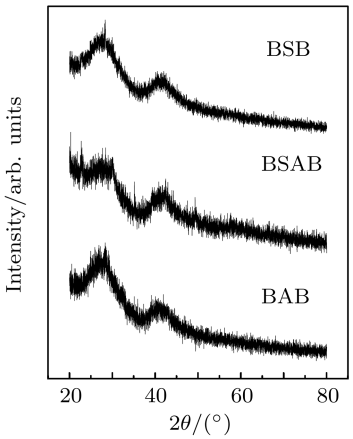


Fig. 3. The XRD patterns of the Er^{3+}-doped 25BaO-(25-x)SiO_2-xAl_2O_3-25B_2O_3 samples for x = 0, 12.5, 25.

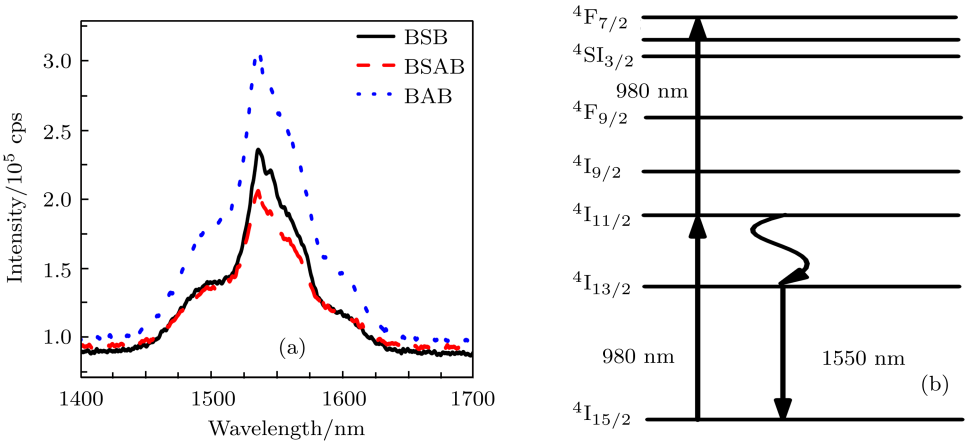


Fig. 4. (colour online) (a) The NIR spectra for different additives of Si and/or Al excited by wavelengths of 980 nm, and (b) the energy level diagram of Er^{3+}.

According to Judd–Ofelt theory,[20,21] the Ω_λ intensity parameters, which can be obtained from absorption or emission spectra, are lattice-dependent for a particular lanthanide ion in different host matrices. The calculated Ω_λ of Er^{3+} ions for all samples from the absorption spectra are summarized in Table 2. It is noted that the symmetric complex network structure shows an obvious relationship with the Si^{4+}/Al^{3+} additive amount. Among the intensity parameters Ω_λ, Ω_2 is more sensitive to the symmetry of the crystal lattice and the covalency of the rare-earth ions with near-neighbour anions.[22] Both of them may exert an influence on the transition probabilities and nonradiative relaxation of the excitation state of rare-earth ions.[23] As revealed by Table 2, Ω_2 gets to a minimum value of 2.866 when Si^{4+} and Al^{3+} are codoped into the glasses, indicating a crystal structure with high symmetry.[24] For the glass with Al^{3+} 25% additive, corresponding to the strong infrared emission at 1540 nm, Ω_2 is at 4.205, which is due to partially broken or forbidden transition for the low symmetry of the crystal field.

Table 2. The calculated intensity parameters of Er^{3+}-doped borate glass.

Samples	Intensity parameters/(10^{-20} cm^2)		
	Ω_2	Ω_4	Ω_6
BSB	3.083	5.645	6.410
BSAB	2.866	2.083	6.318
BAB	4.205	2.198	9.233

To identify the correlation of observed infrared properties and the local environment of the Er^{3+} ions, the Raman spectra of the BSB, BSAB, and BAB glasses are illustrated. Similar spectra are observed for all samples except that an additional band appears at the low-frequency band of 196 cm^{-1} in BSAB and BSB in Fig. 5, ascribing to a possible formation of new groups by Si^{4+} doping. According to Ref. [10], the band peaked at 1510 cm^{-1} originates from the asymmetric stretching mode of borate triangles $[BO_2O]^{-1}$. While the asymmetrical B=O stretching at 1893 cm^{-1} and the B–O–B stretching mode at 1720 cm^{-1} belong to the hexagonal $[B(BO)_4]^{-1}$ group.[25] Also, several small bands at 976 cm^{-1}, 740 cm^{-1}, and 476 cm^{-1} belong to the $[SiO_4]^{-1}$ and $[BSi_4O_{10}]^{-1}$ groups[26] in the BSAB and BSB samples, which are consistent with the position of the endothermic peaks at 682 °C and 735 °C in Fig. 1. The scattering intensity of BAB at 1510 cm^{-1} and 1720 cm^{-1} is twice as strong as that of the other two samples, meaning that more groups of $[BO_2O]^{-1}$ and $[B(BO)_4]^{-1}$ are formed by the addition of Al^{3+}. The difference in this property is governed by Al^{3+} substitution for Si^{4+}, which induces a local charge mismatch[27] and the sequential decline in bond energies of Si–O, B–O, and Al–O.[28] Stretching from the $[BO_2O]^{-1}$ and $[B(BO)_4]^{-1}$ groups yields high-energy vibrations (1510 cm^{-1} and 1720 cm^{-1}, respectively) that cause an increase in the probability of nonradiative relaxation and then a severe change in NIR luminescence intensity.[29]

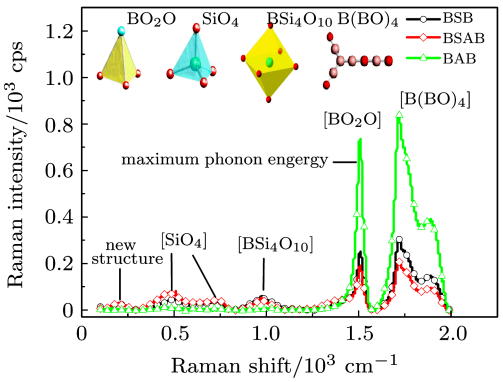


Fig. 5. (colour online) The Raman spectra of borate glass samples for different additions of Si and/or Al. The insets are three-dimensional sketch maps for the main groups $[BO_2O]^{-1}$, $[SiO_4]^{-1}$, $[BSi_4O_{10}]^{-1}$, and $[B(BO)_4]^{-1}$.

In rare-earth glass, the maximum phonon energy of the host could be used for a discussion on multiphonon relaxation, which has an influence on the efficiency of infrared light-emittance.[12,13] Considering the effect of the nonradiative transition process of the intermediate excited state $^4I_{11/2}$ on infrared emission at 1540 nm of Er^{3+}, the nonradiative relaxation probability for the $^4I_{11/2}$–$^4I_{13/2}$ transition can be formulized by[13]

$$W_{\mathrm{NR}} = C\,[n\,(T)+1]^P \exp(-\alpha \Delta E),$$

where exponent P is the phonon order, linking the energy level difference (ΔE) of the $^4I_{11/2}$ level to the next lower energy level $^4I_{13/2}$. $n(T)$, which is correlated with absolute temperature, represents the average vibrational quantum number at 1540 nm. For the maximum phonon energy position of the matrix host, α is denoted as $\hbar\omega_p$, which relates to the ion–phonon coupling. The constant C is dependent on the host and can be expressed as $C \propto \rho(\omega)^{5/3}$.[13] By the choice of maximum phonon energy ω_p, $\rho(\omega_p)$ is the maximum phonon density of state of the matrix. For three samples with different additives of Al^{3+} and/or Si^{4+} doping, the maximum phonon energy value does not change. But there is a significant increase in the maximum phonon density of states in the Al 25% additional sample, corresponding to the highest value of

C. As a result, the $W_{\rm NR}$ value for the Er^{3+} $^4I_{11/2}$ energy level reaches a maximum, resulting in the enhancement of NIR luminescence at 1540 nm.

4. Conclusions

The NIR luminescence properties of Er^{3+} at 1540 nm in borate glass containing Al^{3+} and/or Si^{4+} are investigated. A remarkable intensity enhancement is observed for the sample with an Al additive of 25%. The Judd–Ofelt parameters of the Er^{3+} ions are adopted to explain the intensity change of the NIR fluorescence at 1540 nm. The calculated Judd–Ofelt parameter Ω_2 reaches a maximum value of 4.205, which shows a partially broken forbidden transition for the weak symmetry of the crystal field. The Raman spectra show that the positions of the Raman bands are all similar, but the maximum phonon density of states is completely different. The maximum value of the $W_{\rm NR}$ of the Er^{3+} $^4I_{11/2}$ energy level for the Al 25% addition supports the increase in NIR luminescent intensity at 1540 nm.

References

[1] Pisarski W A, Pisarska J, Lisiecki R, Grobelny L, Grazyna D D, Witold R R 2009 *Opt. Mater.* **31** 1781

[2] Yan X W, Yu H W, Zheng J G, Li M Z, Jiang X Y, Duan W T, Cao D X, Wang M Z, Shan X T and Zhang Y L 2011 *Acta Phys. Sin.* **60** 047801 (in Chinese)

[3] Zhang X S, Li L and Huang Q S 2010 *J. Nanosci. Nanotech.* **10** 5288

[4] Li C R, Li S F, Dong B, Cheng Y Q, Yin H T, Yang J and Chen Y 2011 *Chin. Phys.* B **20** 017803

[5] Rai S and Hazarika S 2008 *Opt. Mater.* **30** 1343

[6] Desirena H, RosaE D, Díaz-Torres L A and Kumar G A 2006 *Opt. Mater.* **28** 560

[7] Reddy A A, Babu S S and Pradeesh K 2011 *J. Alloys Compd.* **509** 4047

[8] Debnath R, Nayak A and Ghosh A 2007 *Chem. Phys. Lett.* **444** 324

[9] Xu S Y, Zhang X S, Zhou Y L, Xi Q and Li L 2011 *Chin. Phys.* B **20** 037804

[10] Lucacel R C and Ardelean I 2007 *J. Non-Cryst. Solids* **353** 2020

[11] Yano T, Kunimine N, Shibata S and Yamane M 2003 *J. Non-Cryst. Solids* **321** 147

[12] Pan Z and Morgan SH 1997 *J. Non-Cryst. Solids* **201** 130

[13] Layne C B, Lowdermilk W H and Weber M J 1977 *Phys. Rev.* B **16** 10

[14] Hirao K, Tanabe S, Kishimoto S, Tamaia K and Sogaa N 1991 *J. Non-Cryst. Solids* **135** 90

[15] Tsang W S, Yu W M and Mak C L 2002 *J. Appl. Phys.* **91** 1871

[16] Gcuil E, Szollosy I and Arnold M 1994 *J. Therm. Anal. Calorim.* **42** 1007

[17] Fatih S, Fatih D and Murat B 2006 *Korean J. Chem. Eng.* **23** 736

[18] Yun Y H and Bray P J 1978 *J. Non-Cryst. Solids* **27** 363

[19] Takashi Y, Hiromitsu F and Hiroshi K 1972 *J. Inorg. Nucl. Chem.* **34** 2739

[20] Ofelt G S 1962 *J. Chem. Phys.* **37** 511

[21] Yao B Q, Zheng L L, Yang X T and Wang T H 2009 *Chin. Phys.* B **18** 1674

[22] Carnall W T, Fields P R and Wybourne B G 1965 *J. Chem. Phys.* **42** 3797

[23] Ebendor H, Ehrta D and Bettinelli M 1998 *J. Non-Cryst. Solids* **240** 66

[24] Tanabe S, Ohyagi T and Soga N 1992 *Phys. Rev.* B **46** 3305

[25] Yao W Z, Guo J C, Lu H G and Li S D 2009 *J. Phys. Chem.* **113** 2561

[26] Song X L, Qu Y X, Xu C and Jiang M H 1998 *Chin. J. Light Scattering* **10** 30

[27] Shao Y W, Ji Z L, Qiang F and Hui N D 2008 *Spectrochim Acta* A **69** 921

[28] Luo Y R 2005 *Handbook of Bond Energics* (Beijing: Science Press) (in Chinese) p. 284

[29] Vetrone F, Boyer J C, Capobianco J A, Speghini A and Bettinelli M 2004 *J. Appl. Phys.* **96** 661